

Atomically resolved 3D structural reconstruction of small Quantum Dots

Pritam Banerjee¹, Chiranjit Roy¹, Juan Jesús Jiménez^{2,3}, Francisco M. Morales^{2,3}, Somnath Bhattacharyya^{1*}

¹Department of Metallurgical and Materials Engineering, Indian Institute of Technology Madras, Chennai, India – 600036

²IMEYMAT: Institute of Research on Electron Microscopy and Materials, University of Cádiz, Spain

³Department of Materials Science and Metallurgic Engineering, and Inorganic Chemistry, Faculty of Sciences, University of Cádiz, Puerto Real, 11510 Cádiz, Spain

* Corresponding author: somnath.iitm@gmail.com

Supplementary information

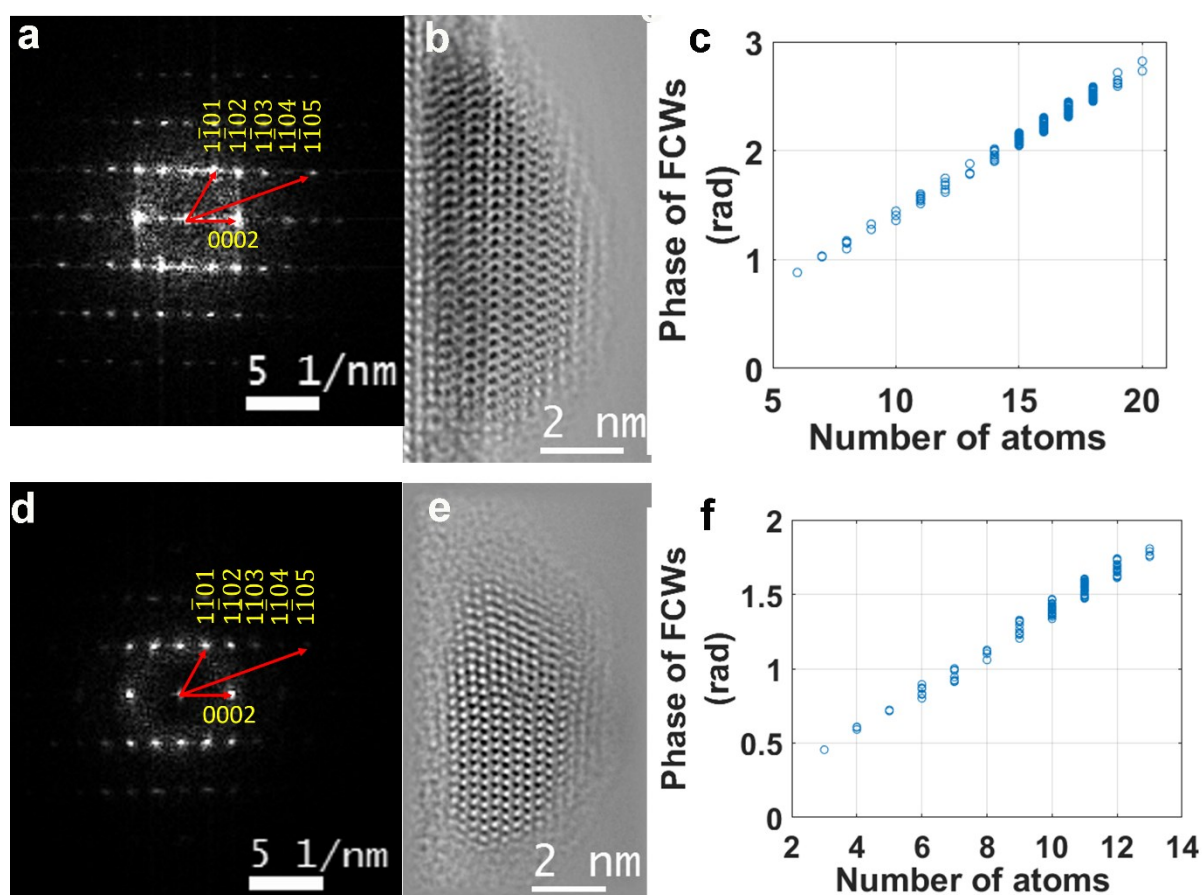


Fig. S1 (a) Power spectrum of the high-resolution lattice image of QD1 in fig. 1(a). (b) Retrieved amplitude from reconstructed exit wave of QD1 (c) Plot of the phase of focus corrected waves vs atom counts for QD1. (d) Power spectrum of the high-resolution lattice image of QD2 in fig. 2(a) (e) Retrieved amplitude from reconstructed exit wave of QD2. (f) Plot of phase of focus corrected waves vs atom counts for QD2.

Procedure of in-line 3D holography

- a. Determination of valley wave or background wave between the atomic columns and propagation of background subtracted wave along the electron beam direction
- b. Determination of exact z height or exit surface geometry using maximum propagated intensity (MPI) criteria
- c. Normalisation of wave at atomic column with valley wave and propagation of normalised wave to exact z height, known as focus correct wave
- d. Measuring the phase value (θ' in rad) between the peak and valley, and plot the difference in the argand plot to construct mass circle
- e. Calculation of phase change (θ in rad) per atom
- f. Finding atom count in each atomic column ($n = \theta' / \theta$) and plotting mass map
- g. Building tomograms using the information of exit surface geometry and number of atoms in each atomic column

Calculation of phase change per atom:

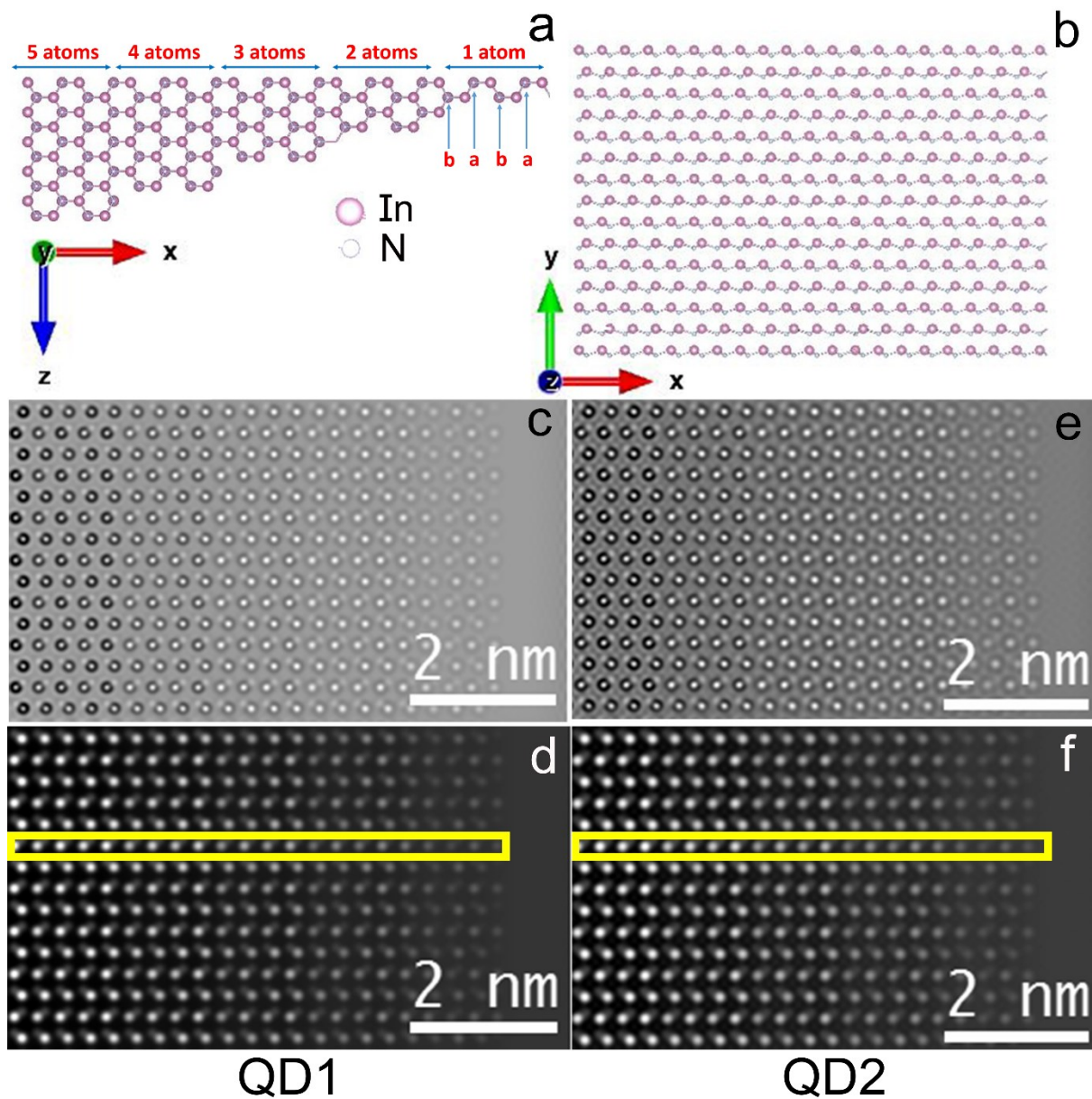


Fig. S2 (a-b) InN wedge shape sample of varying thickness. (c-d) Amplitude and phase of first wedge sample (**parameters same as QD1 imaging**). (e-f) Amplitude and phase of second wedge sample (**parameters same as QD2 imaging**).

The InN wedge shape sample of varying thickness (maximum 5 atoms) was constructed along $[11\bar{2}0]$ direction by VESTA software¹ as shown in fig. S2 a. The wedge sample has

abab stacking along thickness direction. In atom at 'b' layer is placed at half of inter atomic spacing along thickness direction. The top view of the wedge structure is shown in fig. S2 b.

High-resolution images were simulated using a multi-slice algorithm by QSTEM software². The overall sampling and slice thickness was set as 0.25 Å per pixel (same as experimental image) and 0.1 Å respectively.

The imaging parameters for both the experimental QDs were different; therefore we have done two simulations of wedge structure for calculation of phase change per atom.

The imaging parameters for **first wedge (parameters same as QD1 imaging)** are as follows, accelerating voltage = 200 keV, spherical aberration (Cs) = -0.003 mm, Scherzer defocus = 3.4 nm, $g_{\max} = 13 \text{ nm}^{-1}$, Chromatic aberration Cc = 1.4 and energy spread = 0.6 eV. A set of 21 focal series images ranging from defocus -7 nm to -13 nm with a step of 1 nm was used for exit wave reconstruction using FRWR algorithm³.

The imaging parameters for **second wedge (parameters same as QD2 imaging)** are as follows, accelerating voltage = 200 keV, spherical aberration (Cs) = -0.0136 mm, Scherzer defocus = 7.2 nm, $g_{\max} = 10 \text{ nm}^{-1}$, Chromatic aberration Cc = 1.4 and energy spread = 0.6 eV.

A set of 21 focal series images ranging from defocus -2 nm to -17 nm with a step of 1 nm was used for exit wave reconstruction using FRWR algorithm³.

The amplitude and phase of first wedge are shown in fig. S2c and S2d respectively. The amplitude and phase of second wedge are shown in fig. S2e and S2f respectively.

3D structural reconstruction of wedge samples considering only In atomic columns was performed using in-line holography technique⁴. The selected region for 3D reconstruction is shown with yellow rectangle. Step a to d of section 'procedure of inline-3d-holography' was followed for construction of mass circle and calculation of phase of FCWs (θ' rad).

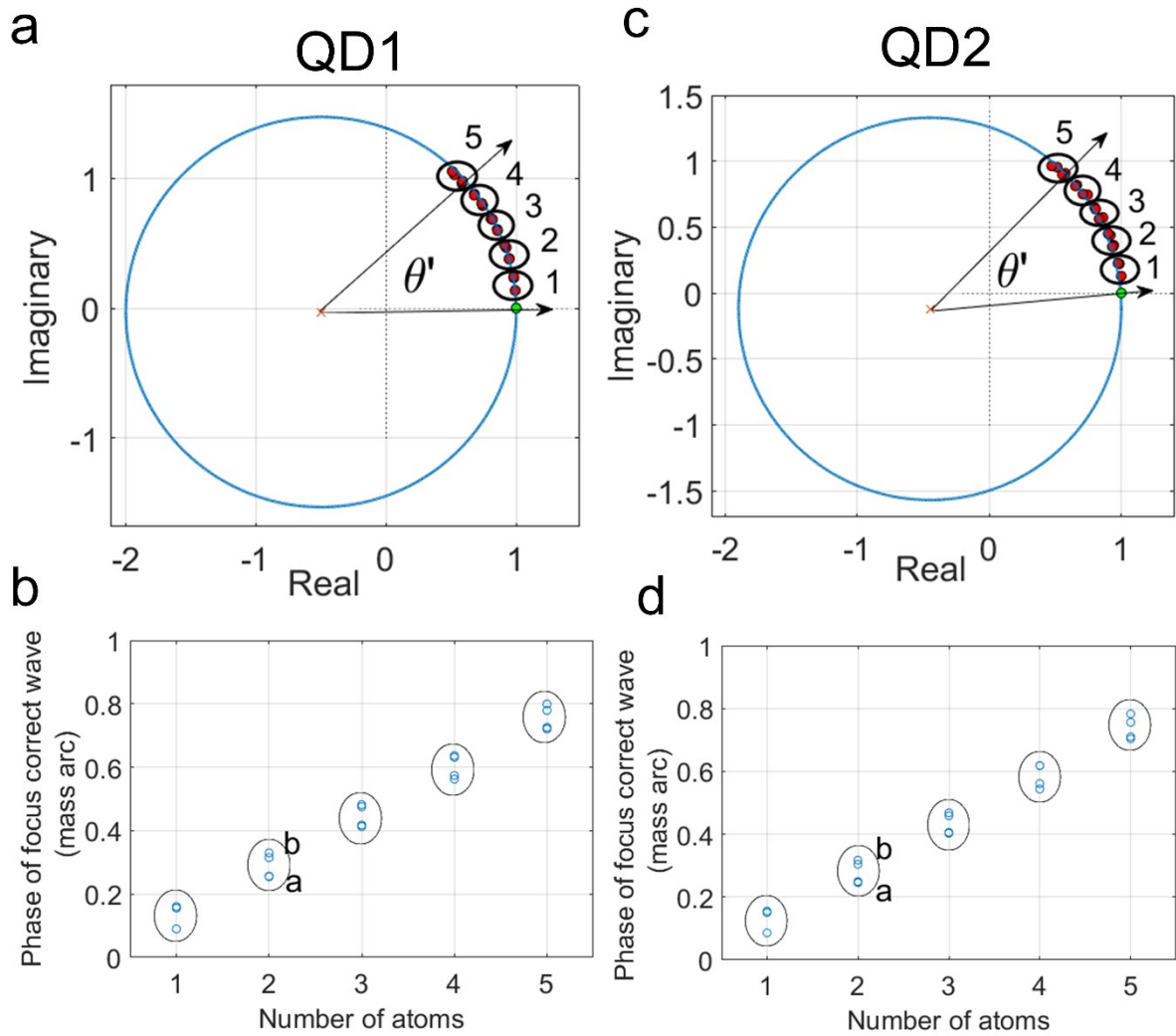


Fig. S3 (a-b) Argand plot and phase of FCWs with atom counts for first wedge structure. (c-d) Argand plot and phase of FCWs with atom counts for second wedge structure.

The argand plots of two wedge samples are shown in fig. S3a and S3c respectively. In both figures, the mass circle consists of pair of mass blobs for each atom count. Each pair of mass blobs represents the In atoms at a and b layer respectively. In atoms are situated at different z height for same atom thickness; therefore atom in “b” layer has only an effective “half potential” of the atom in “a” layer as reported in ref⁵. Hence for single In atom at different layer, we observe different mass blobs in argand plot. The atom count for each pair of mass

blobs is shown in argand plot. The phase of FCWs known as θ' in rad was plotted for each atom counts, as shown in fig. S3b and fig. S3d for wedge1 and wedge2 respectively. Here it is also clear that phase of In atom is different for different stacking layer.

The phase change per atom for each atom count is tabulated in table S1 for both wedge structures. The average and standard deviation of phase change per atom were calculated.

The average phase change per atom was used for 3D reconstruction of experimental QDs.

Table S1: Calculation of phase change per atom using wedge structures

Number of atoms	QD1		QD2	
	Phase of FCW (rad)	phase change per atom (rad)	Phase of FCW (rad)	phase change per atom (rad)
1	0.155594	0.170127	0.149919	0.149919
1	0.089734	0.098118	0.085647	0.085647
1	0.160247	0.175214	0.154639	0.154639
2	0.255132	0.127566	0.245729	0.122865
2	0.314805	0.157403	0.302491	0.151246
2	0.256314	0.128157	0.248159	0.124079
2	0.329684	0.164842	0.315424	0.157712
2	0.254799	0.1274	0.244663	0.122331
3	0.481771	0.16059	0.464619	0.154873
3	0.417499	0.139166	0.400133	0.133378
3	0.47546	0.158487	0.455516	0.151839
3	0.412889	0.13763	0.403293	0.134431
4	0.636366	0.159091	0.6127	0.153175
4	0.562401	0.1406	0.539307	0.134827
4	0.631212	0.157803	0.613658	0.153414
4	0.57374	0.143435	0.55678	0.139195
5	0.779313	0.155863	0.74919	0.149838
5	0.720898	0.14418	0.697624	0.139525
5	0.799255	0.159851	0.775852	0.15517
5	0.725472	0.145094	0.703809	0.140762
	Average	0.147531	Average	0.140443
	Standard deviation	0.017742	Standard deviation	0.016893

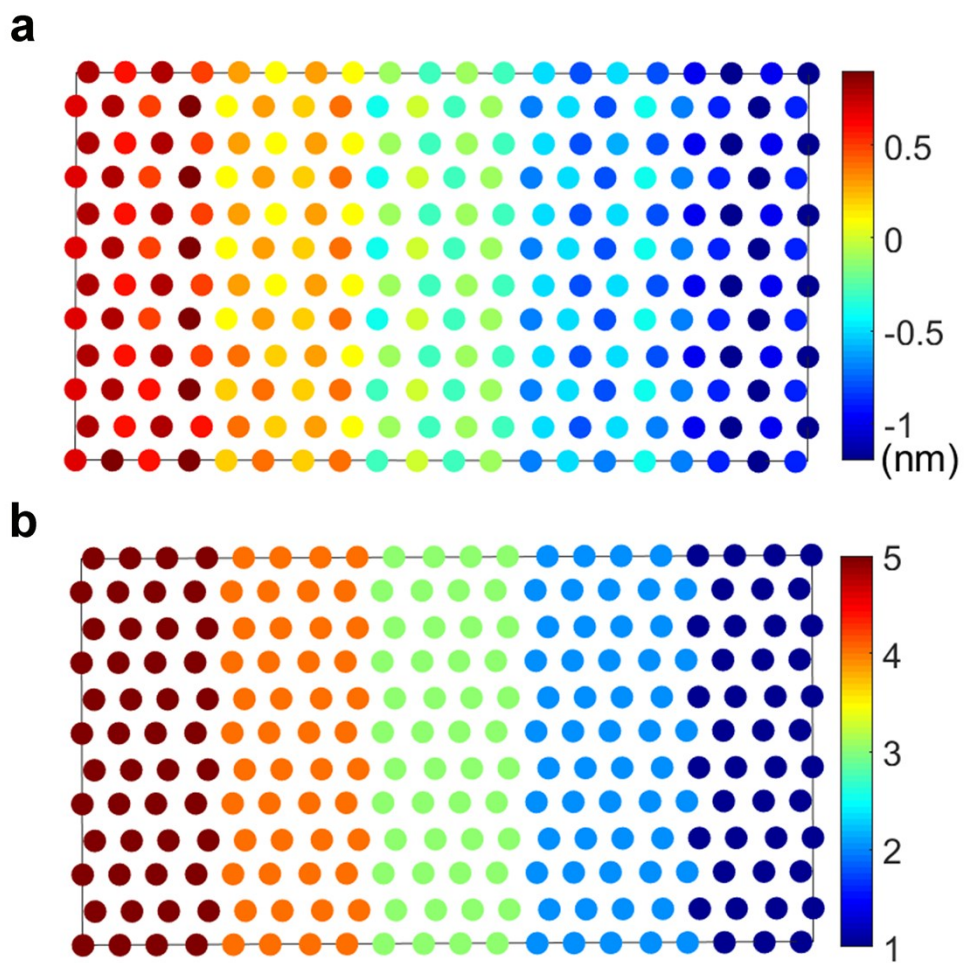


Fig. S4 (a) Defocus map of first InN wedge (parameters same as QD1 imaging) (b) Mass map of first InN wedge sample containing 5 atoms.

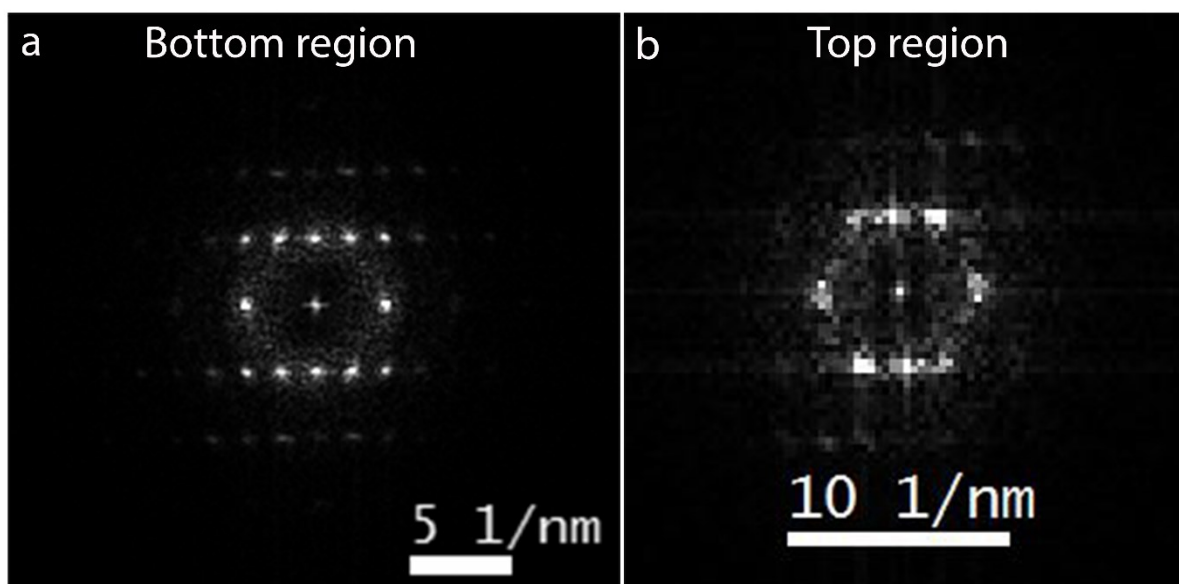


Fig. S5 (a) Power spectrum of bottom region of QD2 (b) Power spectrum of top region of QD2

Table S2: Average and standard deviation of defocus values before and after correction.

Quantum Dot	Curve line	Average defocus (Å)	S.D (Å) Before focus correction	S.D (Å) After focus correction
1	1	-12.45	4.34	2.39
	2	-10.12	3.82	2.08
	3	-13.9	3.12	1.49
	4	-12.28	2.88	1.63
	5	-14.9	3.01	1.72
	6	-13.6	3.16	1.82
	7	-18.25	2.25	1.44
	8	-16.92	3.70	1.31
	9	-19.5	2.62	1.26
2	1	-22.68	5.27	2.50
	2	-27.6	3.52	1.67
	3	-26.42	3.92	1.61
	4	-29.6	3.46	1.96
	5	-26	4.06	2.48
	6	-32	2.93	2.38

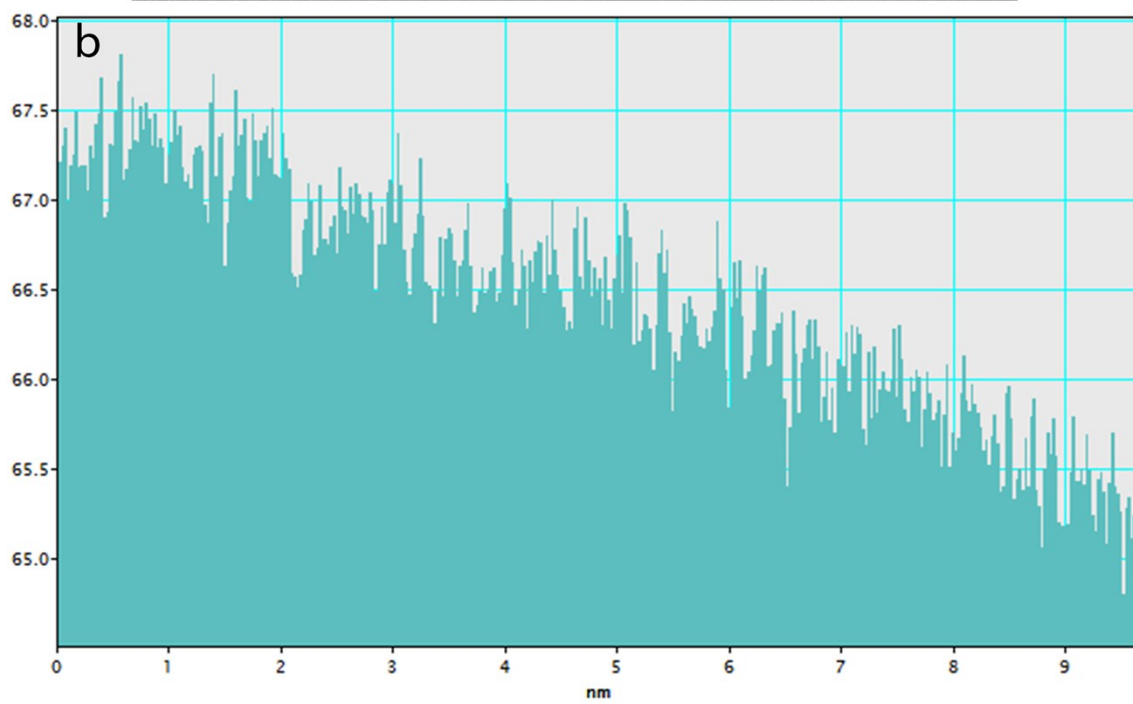
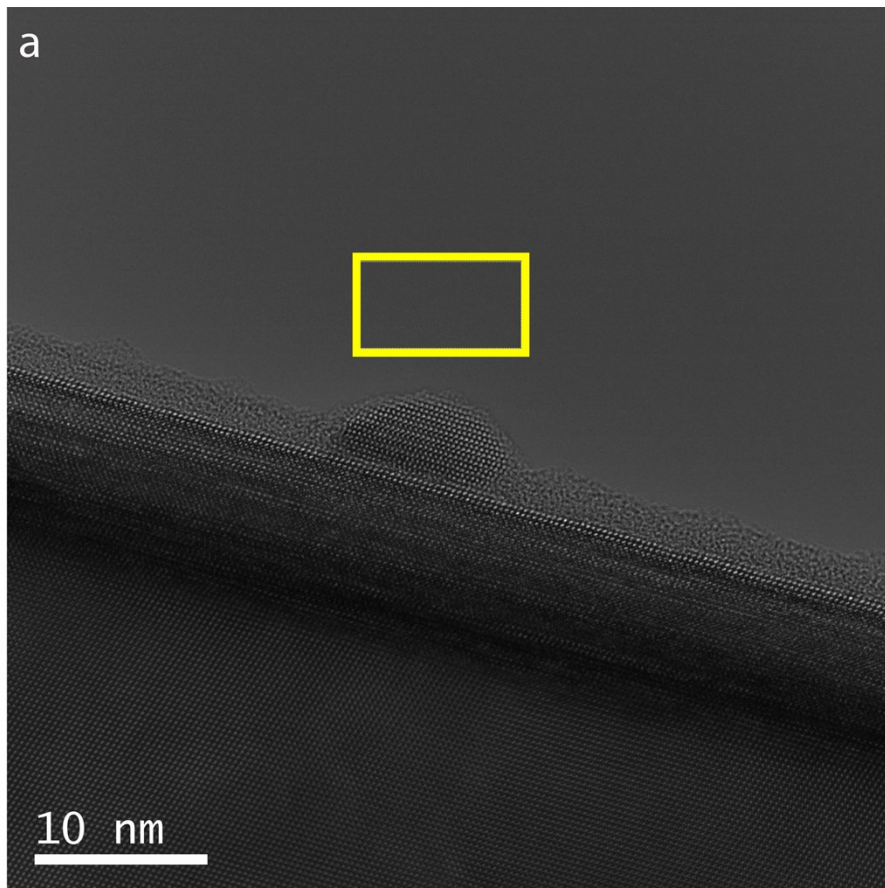


Fig. S6 (a) Lattice image of InN QD1 grown in Si substrate (b) Intensity profile of vacuum region marked by yellow rectangle.

References

- 1 K. Momma and F. Izumi, *J. Appl. Crystallogr.*, , DOI:10.1107/S0021889811038970.
- 2 C. Koch, *Determination of core structure periodicity and point defect density along dislocations*, Arizona State University, 2002.
- 3 C. T. Koch, *Ultramicroscopy*, 2008, **108**, 141–150.
- 4 F. R. Chen, D. Van Dyck and C. Kisielowski, *Nat. Commun.*, 2016, **7**, 462–463.
- 5 F.-R. Chen, C. Kisielowski and D. Van Dyck, *Micron*, 2015, **68**, 59–65.